Mass-radius relation for neutron stars in $f(R)$ gravity

Salvatore Capozziello,[1,2,3,*] Mariafelicia De Laurentis,[4,5,6,2,†] Ruben Farinelli,[7,‡] and Sergei D. Odintsov[8,9,§]

[1]*Dipartimento di Fisica, Universitá di Napoli "Federico II," Compl. Univ. di Monte S. Angelo,
Edificio G, Via Cinthia, I-80126 Napoli, Italy*
[2]*INFN Sezione di Napoli, Compl. Univ. di Monte S. Angelo, Edificio G, Via Cinthia, I-80126 Napoli, Italy*
[3]*Gran Sasso Science Institute (INFN), Via F. Crispi 7, I-67100 L' Aquila, Italy*
[4]*Institut für Theoretische Physik, Goethe-Universität, Max-von-Laue-Str. 1, 60438 Frankfurt, Germany*
[5]*Tomsk State Pedagogical University, ul. Kievskaya, 60, 634061 Tomsk, Russia*
[6]*Lab. Theor. Cosmology, Tomsk State University of Control Systems and Radioelectronics (TUSUR),
634050 Tomsk, Russia*
[7]*ISDC Data Center for Astrophysics, Université de Genève,
chemin d'Écogia 16, 1290 Versoix, Switzerland*
[8]*Instituciò Catalana de Recerca i Estudis Avançats (ICREA), Passeig de Lluís Companys 23, 08010
Barcelona, Spain*
[9]*Institut de Ciencies de l'Espai (IEEC-CSIC), Campus UAB, Torre C5-Par-2a pl,
E-08193 Bellaterra, Barcelona, Spain*

We discuss the mass-radius diagram for static neutron star models obtained by the numerical solution of modified Tolman-Oppenheimer-Volkoff equations in $f(R)$ gravity where the Lagrangians $f(R) = R + \alpha R^2(1 + \gamma R)$ and $f(R) = R^{1+\epsilon}$ are adopted. Unlike the case of the perturbative approach previously reported, the solutions are constrained by the presence of an extra degree of freedom, coming from the trace of the field equations. In particular, the stiffness of the equation of state determines an upper limit on the central density ρ_c above which the positivity condition of energy-matter tensor trace $T^m = \rho - 3p$ holds. In the case of quadratic $f(R)$ gravity, we find higher masses and radii at lower central densities with an inversion of the behavior around a pivoting ρ_c which depends on the choice of the equation of state. When considering the cubic corrections, we find solutions converging to the required asymptotic behavior of the flat metric only for $\gamma < 0$. A similar analysis is performed for $f(R) = R^{1+\epsilon}$ considering ϵ as the leading parameter. We work strictly in the Jordan frame in order to consider matter minimally coupled with respect to geometry. This fact allows us to avoid ambiguities that could emerge in adopting the Einstein frame.

I. INTRODUCTION

The structure of a neutron star (NS) is strictly correlated with the equation of state (EoS), i.e. the relation between pressure and density in its interior [1]. Given an EoS, a mass-radius $(M - \mathcal{R})$ relation and a corresponding maximal mass can be derived, in principle, for any NS. Furthermore the knowledge of these parameters provides significant information related to the mechanism responsible for NS formation and possible effects on the evolutionary history of their progenitors. For an introduction to the theory of relativistic stars, see for example [2].

Up to now, the physical properties of matter in strong gravity regimes have been studied only by considering theoretical models since it is not possible to produce similar environments in the laboratory. Due to this situation, there are more than 100 candidates for the EoS, but only some of

them should be reliable once observational probes fix them. Consequently, the measurement of NS masses is thus important for our understanding on the matter behavior in extreme regimes. Beside these considerations, it is well known that Chandrasekhar, considering degenerate matter, fixed a theoretical upper limit for the stability of a non-rotating NS at $1.44M_\odot$ [3]. From an observational point of view, the determination of mass can be achieved with accuracy only for NSs in binary systems. In particular, the most accurate mass measurements have been derived for the binary radio pulsars where values of masses are around $1.35M_\odot$ [4]. However, for the x-ray pulsar Vela X-1, it has been measured at a mass of the order $1.86 \pm 0.16M_\odot$ [5,6] and, for 4U 1822-371, a mass of the order $2M_\odot$ [7]. More massive NSs were discovered, such as the millisecond radio pulsar $J0751 + 1807$ with a measured mass of $2.1 \pm 0.2M_\odot$ [8]. Furthermore, the pulsar PSR $J1614 - 2230$ [9] has set rigid constraints on various EoSs at strong density regimes. In summary, the mass of a NS cannot exceed the maximal mass limit in the range $3.2 - 3.6M_\odot$ according to general relativity (GR) [10,11]. It is important

[*]capozzie@na.infn.it
[†]mfdelaurentis@tspu.edu.ru
[‡]ruben.farinelli@gmail.com
[§]odintsov@ieec.uab.es

to stress that these limits on maximal mass exclude many EoS according to the observational data. Therefore, since different assumptions provided different results, we can say that the actual mass limit for NS is still a mystery. We need a more accurate derivation consistent with the observations. In other words, this state of the art allows us to assume that the NS mass should be in the range $1.4M_\odot$ to $6M_\odot$. This situation is very unsatisfactory and so there is a severe need for reliable methods to obtain the NS mass limit; otherwise we are waiting for more precise observations.

In this paper we will face the problem of the NS mass limit adopting $f(R)$ gravity. This is a straightforward extension of GR where one relaxes the strict request that the gravity action is linear in the Ricci scalar R as in the Hilbert-Einstein case. These models can be seen as simple cases of a more general class of extended theories of gravity [12–19]. The reason why we adopt such an approach is that higher order curvature corrections can emerge in the extreme gravity regimes inside a NS [20–23]. The effective pressure related to the curvature could naturally cure, in principle, some shortcomings of NS theory that are often addressed by asking for exotic EoSs [20]. The philosophy of the present paper is to construct reliable $M - \mathcal{R}$ relations solving directly the full modified Tolman-Oppenheimer-Volkoff (TOV) system equations [24]. In other words, in our numerical integrations, we are not imposing arbitrary perturbation methods but solving numerically the full TOV system. In particular, we take into account quadratic and cubic corrections to the Ricci scalar and, in general, power-law $f(R)$ models. The aim is to control precisely how the results deviate from those of GR in order to see where strong gravity regimes emerge and affect the $M - \mathcal{R}$ relation.

The paper is organized as follows: In Sec. II, we derive the modified TOV equations for $f(R)$ gravity. In particular, we consider $f(R)$ models with quadratic and cubic corrections and generic power law $f(R)$ models. Solutions of stellar structure equations are given in Sec. III. In Sec. IV, we discuss the results, focusing, in particular, on the $M - \mathcal{R}$ relation. Conclusions and discussion are reported in Sec. V. Through the paper, we will indicate with $\mathcal{R}$ the radius of the object and with R the Ricci curvature scalar.

II. TOLMAN-OPPENHEIMER-VOLKOFF EQUATIONS FOR $f(R)$ GRAVITY

Let us start from the $f(R)$ action given by

$$\mathcal{A} = \frac{c^4}{16\pi G}\int d^4x\sqrt{-g}[f(R) + \mathcal{L}_{\text{matter}}], \quad (1)$$

where g is the determinant of the metric $g_{\mu\nu}$ and $\mathcal{L}_{\text{matter}}$ is the standard perfect fluid matter Lagrangian. The variation of (1) with respect to $g_{\mu\nu}$ gives the field equations [12–19]

$$\frac{df(R)}{dR}R_{\mu\nu} - \frac{1}{2}f(R)g_{\mu\nu} - [\nabla_\mu\nabla_\nu - g_{\mu\nu}\Box]\frac{df(R)}{dR} = \frac{8\pi G}{c^4}T_{\mu\nu}, \quad (2)$$

where $T_{\mu\nu} = \frac{-2}{\sqrt{-g}}\frac{\delta(\sqrt{-g}\mathcal{L}_m)}{\delta g^{\mu\nu}}$ is the energy momentum tensor of matter. Here we adopt the signature $(+,-,-,-)$. The metric for systems with spherical symmetry has the usual form

$$ds^2 = e^{2w}c^2dt^2 - e^{2\lambda}dr^2 - r^2(d\theta^2 + \sin^2\theta d\phi^2), \quad (3)$$

where w and λ are functions depending only on the radial coordinate r. Within the star, matter is described as a perfect fluid, whose energy-momentum tensor is $T_{\mu\nu} = \text{diag}(e^{2w}\rho c^2, e^{2\lambda}p, r^2p, r^2p\sin^2\theta)$, where ρ is the matter density and p is the pressure [25]. The equations for the stellar configuration are obtained adding the condition of hydrostatic equilibrium which can be derived from the contracted Bianchi identities

$$\nabla^\mu T_{\mu\nu} = 0, \quad (4)$$

that give the Euler conservation equation

$$\frac{dp}{dr} = -(\rho + p)\frac{dw}{dr}. \quad (5)$$

From the metric (3) and the field equations (2), it is possible to derive the equations for the functions λ and w in the form [26]

$$\frac{d\lambda}{dr} = \frac{8e^{2\lambda}G\pi r\rho}{c^2(2\frac{df}{dR} + rR'\frac{d^2f}{dR^2})} + \frac{e^{2\lambda}[(r^2R - 2)\frac{df}{dR} - fr^2]}{2r(2\frac{df}{dR} + rR'\frac{d^2f}{dR^2})}$$
$$+ \frac{\frac{df}{dR} + r[\frac{d^2f}{dR^2}(2R' + rR'') + rR'^2\frac{d^3f}{dR^3}]}{r(2\frac{df}{dR} + rR'\frac{d^2f}{dR^2})}, \quad (6)$$

and

$$\frac{dw}{dr} = \frac{8e^{2\lambda}GP\pi r}{c^4(2\frac{df}{dR} + rR'\frac{d^2f}{dR^2})}$$
$$+ \frac{e^{2\lambda}[fr^2 + (2 - r^2R)\frac{df}{dR}] - 2(\frac{df}{dR} + 2rR'\frac{d^2f}{dR^2})}{2r(2\frac{df}{dR} + rR'\frac{d^2f}{dR^2})}, \quad (7)$$

respectively. In both Eqs. (6) and (7), the prime denotes a derivative with respect to r for the Ricci scalar $R(r)$.

The above equations are the modified TOV equations that, for $f(R) = R$, reduce to the standard TOV equations of GR [27,28]. It is important to stress that, in $f(R)$ gravity, the Ricci scalar is a dynamical variable and then we need a

further equation to solve the system of equations (5), (6) and (7). For this aim one needs to consider the trace of the field equations (2) which takes the form

$$3\Box \frac{df(R)}{dR} + \frac{df(R)}{dR}R - 2f(R) = \frac{8\pi G}{c^4}(\rho - 3p), \quad (8)$$

where

$$\Box = \frac{1}{\sqrt{-g}}\frac{\partial}{\partial x^\nu}\left(\sqrt{-g}g^{\mu\nu}\frac{\partial}{\partial x^\mu}\right) \quad (9)$$

is the d'Alembert operator in curved spacetime. It can be easily checked that for $f(R) = R$, Eq. (8) reduces to the trace of GR, i.e.

$$R = -\frac{8\pi G}{c^4}(\rho - 3p). \quad (10)$$

In order to close the system of Eqs. (5)–(8), one needs to provide an EoS, $P(\rho)$, relating the pressure and the density inside the star.

In the next subsection we will take into account two physically relevant $f(R)$ Lagrangians with the aim to obtain the $M - \mathcal{R}$ diagram for NS. We use a fully self-consistent nonperturbative approach to solve the stellar-structure equation in their *exact* form.

A. The case $f(R) = R + \alpha R^2(1 + \gamma R)$

We first consider here a quadratic form of $f(R)$ with cubic corrections, according to

$$f(R) = R + \alpha R^2(1 + \gamma R), \quad (11)$$

where both α and γ have dimensions cm^{-2}. This class of models can be related to the presence of strong gravitational fields and emerge, for example, in cosmology, to achieve inflation. In particular higher-derivative curvature terms naturally lead to the cosmic accelerated expansion of inflation [29]. At a fundamental level, their origin is related to the effective actions coming from quantum gravity [30] or from quantum field theory formulated in curved space-time [31]. They lead to renormalizable models at the one-loop level. In the extreme gravity regime of NS, also if very far from the full quantum gravity regime, it is realistic to suppose the emergence of curvature corrections to improve the pressure effects. It is important to stress that such a model cannot be confronted with the Solar System tests of GR since the quadratic and cubic terms emerge in the strong gravity regime as discussed above. They cannot be present at Solar System scales since the only relevant term in the weak field regime is the linear Ricci scalar R. The interest of this model, in the present context, is that the interior of a NS is a natural laboratory where high curvature regimes can emerge and lead to the $M - \mathcal{R}$ relation (see also the discussion in [20]). In some sense, the interior of a NS is similar to the conditions of the early Universe.

For this model, Eqs. (6) and (7) take the form

$$\frac{d\lambda}{dr} = \frac{4e^{2\lambda}G\pi r\rho}{c^2[1 + R\alpha(2 + 3R\gamma) + r\alpha(1 + 3R\gamma)R']}$$
$$+ \frac{1}{4r[1 + R\alpha(2 + 3R\gamma) + r\alpha(1 + 3R\gamma)R']}$$
$$\times \{e^{2\lambda}[R\alpha(R(r^2 - 6\gamma + 2r^2R\gamma) - 4) - 2]$$
$$+ 2[1 + 3R^2\alpha\gamma + 2r\alpha(R'(2 + 3\gamma R') + rR'')]$$
$$+ 4R\alpha[1 + 3r\gamma(2R' + rR'')]\}, \quad (12)$$

and

$$\frac{dw}{dr} = \frac{4e^{2\lambda}GP\pi r}{[c^4(1 + R\alpha(2 + 3R\gamma) + r\alpha(1 + 3R\gamma)R']}$$
$$+ \frac{1}{4r[1 + R\alpha(2 + 3R\gamma) + r\alpha(1 + 3R\gamma)R']}$$
$$\times e^{2\lambda}[2 + R\alpha(4 - R(r^2 - 6\gamma + 2r^2R\gamma))]$$
$$- 2[1 + R\alpha(2 + 3R\gamma) + 4r\alpha(1 + 3R\gamma)R'], \quad (13)$$

while the trace Eq. (8) becomes

$$\frac{d^2R}{dr^2} = \frac{1}{6c^4r\alpha(1 + 3R\gamma)}$$
$$\times e^{2\lambda}r[c^4R(R^2\alpha\gamma - 1) + 8G\pi(-3P + c^2\rho)]$$
$$- 6c^4\alpha R'[3r\gamma R' + (1 + 3R\gamma)(2 + rw' - r\lambda')]. \quad (14)$$

B. The case $f(R) = R^{1+\epsilon}$

Another interesting class is

$$f(R) = R^{1+\epsilon}, \quad (15)$$

that are power-law models. If we assume small deviation with respect to GR, that is $|\epsilon| \ll 1$, it is possible to write a first-order Taylor expansion as

$$R^{1+\epsilon} \simeq R + \epsilon R \log R + O(\epsilon^2), \quad (16)$$

which is interesting in order to define the right physical dimensions of the coupling constant and to control the magnitude of the corrections with respect to the standard Einstein gravity. A Lagrangian form like that in Eq. (16) has been widely tested giving interesting results starting from the Solar System up to cosmological scales. Applications have been found in the case of the cosmological background of gravitational waves [32], or in comparing the effects of small deviations on the apsidal motion of a sample of eccentric eclipsing detached binary stars [33]. Very strong bounds have been worked out from null and timelike geodesics in case of the Solar System

[34]. Furthermore, black hole solutions using also the Noether symmetry approach have been found for this kind of Lagrangian [35,36]. The interest of these models is related to the fact that the value of the parameter ϵ can straightforwardly relate a weak field curvature regime ($\epsilon \simeq 0$) to a regime where strong curvature effects start to become relevant ($\epsilon \neq 0$). In fact, as shown in [34], the Solar System constraints give essentially $\epsilon \to 0$. This is not the case for NS where high curvature regimes are very far from the Solar System weak field limits. In this perspective, ϵ could be different from zero in NS and then probe deviations with respect to GR. In this sense, NS could constitute a formidable test for alternative gravity.

The explicit forms of Eqs. (6) and (7) for the action (16) take the form

$$\frac{d\lambda}{dr} = \frac{8e^{2\lambda}G\pi rR\rho}{c^2[2R(1+\varepsilon+\varepsilon\log R)+r\varepsilon R']}$$
$$+ \frac{1}{2rR[2R(1+\varepsilon+\varepsilon\log R)+r\varepsilon R']}$$
$$\times \{e^{2\lambda}R^2[r^2R\varepsilon-2(1+\varepsilon+\varepsilon\log R)]$$
$$+ 2[R^2(1+\varepsilon+\varepsilon\log R)-r^2\varepsilon R'^2+rR\varepsilon(2R'+rR'')]\},$$
$$(17)$$

and

$$\frac{dw}{dr} = \frac{8e^{2\lambda}GP\pi rR}{c^4[2R(1+\varepsilon+\varepsilon\log R)+r\varepsilon R']}$$
$$- \frac{1}{2r[2R(1+\varepsilon+\varepsilon\log R)+r\varepsilon R']}$$
$$\times \{e^{2\lambda}R[r^2R\varepsilon-2(1+\varepsilon+\varepsilon\log R)]$$
$$+ 2[R(1+\varepsilon+\varepsilon\log R)+2r\varepsilon R']\}, \quad (18)$$

while the trace equation is given by

$$\frac{d^2R}{dr^2} = \frac{R'^2}{R} + R'\left(\lambda'-\frac{2}{r}-w'\right)$$
$$- \frac{e^{2\lambda}R[c^4R(1-\varepsilon)+8G\pi(3P-c^2\rho)+c^4R\varepsilon\log R]}{3c^4\varepsilon}.$$
$$(19)$$

In the framework of these models, let us now discuss the stellar structure for these models with the aim to achieve the $M-\mathcal{R}$ relation for some physically relevant EoS.

III. THE STELLAR STRUCTURE EQUATIONS

Let us consider dimensionless variables for solving the system of equations (5)–(8). We set the definitions $x = r/r_g$, $\hat{R} = Rr_g^2$, $p = P/P_0$, $\hat{\rho} = \rho/\rho_0$, where $r_g = GM_\odot/c^2$, $P_0 = M_\odot c^2/r_g^3$ and $\rho_0 = M_\odot/r_g^3$, where $r_g = 1.48 \times 10^5$ cm. By the substitution $R' = q$, the trace

equation for R is lowered by an order of derivation, and the full set of equations is reduced to a system of first-order ordinary differential equations, which can be expressed as

$$\lambda' = F_1(\lambda, w, w', R, q, q', p, x),$$
$$w' = F_2(\lambda, \lambda', w', R, q, q', p, x),$$
$$R' = F_3(q, x),$$
$$q' = F_4(\lambda, \lambda', w, w', R, q, p, x),$$
$$p' = F_5(w', p, x). \quad (20)$$

In such a way, we can deal with the stellar structure equations under the standard of dynamical systems (see also [21]).

The requirement of asymptotic flatness for the metric implies that $\lambda \to 0$, $w \to 0$, $R \to 0$ for $r \to \infty$. The boundary value problem (BVP) can be reduced to an initial value problem (IVP) by imposing initial conditions at the star center $x = 0$ such that the function asymptotically has the needed behavior. For the pressure, the condition is simply $p(0) = p_c$, where p_c is determined by the chosen EoS once the central density ρ_c is fixed. For the remaining functions, the problems deserve some considerations: first of all, we notice that the natural initial conditions for λ and the Ricci scalar are $\lambda(0) = 0$ and $R'(0) = 0$. On the other hand, it is worth pointing out that the potential function w appears in Eqs (5)–(8) only through its first and second derivatives w' and w''. This means that its initial value $w(0)$ can be defined up to an arbitrary constant. Once the full solution is obtained, the value of w at the star center can be shifted *a posteriori* such that $w \to 0$ asymptotically.

The most critical point for the numerical solutions concerns the value of the Ricci scalar at the center. In the classical version of the *shooting method*, the right initial value of R_0 is given by the root of the function $F(R_0) = y(R_0, x_{\max}) - R^b(x_{\max})$, where $y(R_0, x_{\max})$ is the value of R at the boundary of the domain obtained with the initial condition R_0, while $R^b(x_{\max})$ is the imposed boundary condition (BC). Once they are provided with an initial guess for R_0, algorithms for root searching, such as the Newton method for quadratic convergence, give the initial values, if they are not too far from the solutions.

The implicit assumptions of the shooting method however are that the function $y(R_0, x_{\max})$, and in turn $F(R_0)$, is defined for any R_0; moreover the classical computation requires us to determine numerically the derivative dy/dR_0 at each iteration.

In our case, this approach has not been possible for two reasons: first of all, for some initial guess values of R_0, smaller than the right one, the function R at some distance $x > x_{\text{crit}}$ becomes negative, leading to unphysical solutions for the system of equations (5)–(8). Additionally, the numerical computation of the derivative dy/dR_0 at $x_{\max}$ becomes time consuming and strongly ill conditioned,

depending critically on the choice of the step size for R_0. The latter problem originates because of the diverging behavior of the negative R-function at values progressively higher than x_{crit}.

We thus implemented a different method as follows: we first define for R_0 an initial guess interval $R_0^{\min} \approx R_0/5$ and $R_0^{\max} \approx 5R_0$, where $R_0 = 8\pi(\rho_c - 3p_c)$ is the GR value. Then we use a bisection method over the given interval, which allows us to get progressively closer to the right value of R_0 through subsequent interval subdivisions. The iteration stops when a further interval subdivision does not produce appreciable change at $R(x_{\max})$. The needed accuracy in the determination of R_0 depends on the form of $f(R)$ and its variable parameters. In the case of $f(R) = R + \alpha R^2(1 + \gamma R)$, we found that, for all considered values of α, the fine-tuning needs to be very tight, independently of the value of γ.

However, the bisection procedure over the initial interval of R_0-values allows us to achieve a precision as high as desired, which is in fact limited only by the numerical accuracy of the integration routines. In general, a few tens of iterations are required leading to the determination of R_0 with a precision of order $\Delta R_0/R_0 < 10^{-7}$. For the Lagrangian $f(R) = R^{1+\varepsilon}$, on the other hand, as ε gets progressively closer to zero, the results become much less sensitive to R_0; namely, $R_0 = kR_0^{\text{GR}}$, with k of the order 2, gives the same stellar masses and radii. In this case we considered the value $R_0 = 1/2(R_0^{\min} + R_0^{\max})$. The adimensional NS radius is defined by the condition $p(x_{\text{ns}}) = 0$; for $x > x_{\text{ns}}$ the integration is continued in vacuum for the metric potentials λ and w, and for the Ricci scalar R.

To check the accuracy of the results, we tested both a Gear $M = 2$ method and fourth-order Runge-Kutta method with adaptive step size and accuracy control of the functions during the integration of the set of above differential equations (see [37] for details); we found no significant differences between the two methods. Finally, the gravitational mass is obtained *a posteriori* by using a Gauss-Legendre quadrature rule for the integral

$$M_{\text{grav}} = \rho_0 r_g^3 \int_0^{x_{\text{ns}}} 4\pi x^2 \rho(x)dx, \qquad (21)$$

where x_{ns} is the adimensional NS radius, while $\rho(x)$ is obtained by computing the inverse of the function $p(\rho)$ of the EoS.

IV. RESULTS

As previously mentioned, the stellar structure equations require us to specify the EoS relating the matter pressure and density. From a mathematical point of view, the EoS is the algebraic relation needed to close the system. There is however an important point to keep in mind that has been surprisingly little discussed in literature, namely the maximal density ρ_c at the center of the star which can be used in numerical simulations.

Depending on the stiffness of the EoS, the maximum implementable value of ρ_c is given by the need to preserve the physical condition $Tr(T) = \rho_c c^2 - 3P_c > 0$ for the trace equation. In the standard TOV system or in the perturbative approach, $Tr(T)$ does not appear explicitly in the equations of the stellar structure. However in the exact treatment, $Tr(T)$ represents the source term in the right-hand side of the trace equation differential operator [see Eq. (8)]. Values of ρ_c violating its positivity lead to unphysical results. As a consequence, the top-left extension of the branches of $M - \mathcal{R}$ diagrams is limited by the maximum achievable value of ρ_c preserving the positivity of the energy-matter tensor for a given EoS. This limits of course the possibility to investigate the stability of compact stellar structures up to arbitrary central density values. In this paper, we used the analytical representation of EoS with different stiffnesses as reported in [38–40] (labeled as BSk19, BSk20 and BSk21) and the SLy EoS reported in [41]. The maximum allowed central densities in units of 10^{15} gr/cm^3 are $\rho_c = 2$, 1.25, 1.35, 1.7 for EoS BSk19, BSk20, BSk21 and SLy, respectively.

A. Results for $f(R) = R + \alpha R^2$

We first considered quadratic $f(R)$ gravity as reported in Eq. (11) with $\gamma = 0$ and progressively increasing values of α. Note that it has to be $\alpha < 0$ because of the adopted sign convection of the metric signature [see Eq. (3)]. Adopting negative α, we are avoiding ghost modes and instability behaviors [42]. An example of the radial behavior of the metric potentials λ and w, the Ricci scalar R and the pressure P is shown in Fig. 1.

The $M - \mathcal{R}$ diagrams obtained for the four different EoSs here considered are instead shown in Fig. 2, together with the solution of the classical TOV $(\alpha = 0)$. Independently of the EoS, as $|\alpha|$ increases, the following behavior can be observed: the masses at lower central density are higher; then the branch crosses the classical GR solution and for $\rho_c > \rho_c^{\text{crit}}$, $M_{f(R)} < M_{\text{GR}}$. The value of ρ_c^{crit} depends on the EoS, and it is approximatively $0.6 \times 10^{15} < \rho_c^{\text{crit}} < 1 \times 10^{15}$ (Fig. 3). The results reported in Figs. 2 and 3 are obtained for values up to $|\alpha| = 20$. Further higher values produce additional *counterclockwise* rotation of the $M - \mathcal{R}$ traces, until getting a saturation for $|\alpha| > 100$. There is an anticorrelation between α and the required value of the Ricci scalar R_0 at the NS center simultaneously satisfying the asymptotic condition $R \rightarrow 0$. This can be qualitatively understood also looking at the trace of the field equations in quadratic $f(R)$ gravity, which can be written as
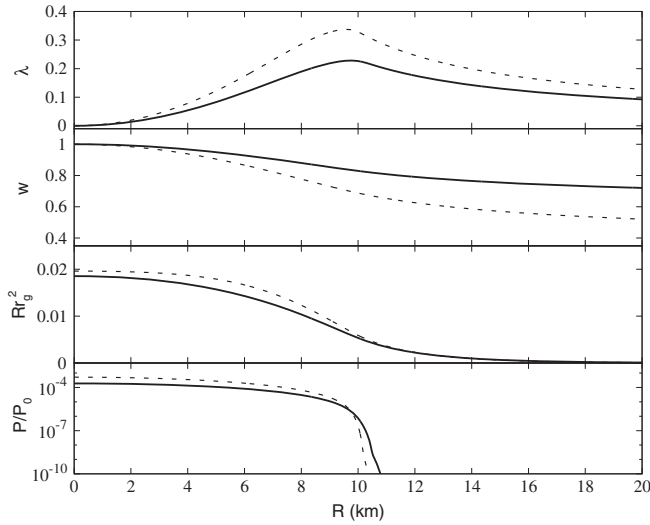
$$\Box R + m^2(R + \chi T) = 0, \qquad (22)$$

FIG. 1. Radial profile for the metric potentials λ and $|w|$, the dimensionless Ricci scalar $\hat{R} = Rr_g^2$ and the dimensionless pressure P/P_0, obtained from the solution of the system of equations (5), (12), (13), and (14) for $f(R) = R + \alpha R^2$ with $|\alpha| = 1$. The central densities reported are $\rho_c = 1 \times 10^{15}$ gr/cm^3 (thick line) and $\rho_c = 1.5 \times 10^{15}$ gr/cm^3 (dashed line), for the Eos BSk19.

where $m^2 = -\frac{1}{6\alpha}$ is an effective mass, $\chi = \frac{8\pi G}{c^4}$ and, in vacuum, the R-function exponentially decays approximatively as e^{-mr}. The higher the value of $|\alpha|$, the higher is the distance at which the Ricci scalar asymptotically goes to zero. A function obeying the condition $R'(0) = 0$ and the asymptotic zero-value condition at large radii needs to be smaller at $r = 0$ when the exponential-decay constant m decreases.

B. Results for $f(R) = R + \alpha R^2(1 + \gamma R)$

Let us improve now the above considerations by taking into account $f(R)$ models with a nonzero cubic correction term with $\gamma \neq 0$ in the Lagrangian (11). It is also evident that the higher the value of $|\alpha|$, the higher must be the value of $|\gamma|$ in order to see appreciable deviations from quadratic $f(R)$ gravity. We discuss here the case $|\alpha| = 0.5$ as an example, showing the results in Fig. 4 for the case of a SLy EoS. For positive and progressively increasing values of γ, the behavior of the traces in the $M - \mathcal{R}$ diagram is similar to that of the quadratic $f(R)$ form at increasing values of $|\alpha|$: higher masses and radii below a certain central density ρ_c and inversion of the trend above it. These results can be
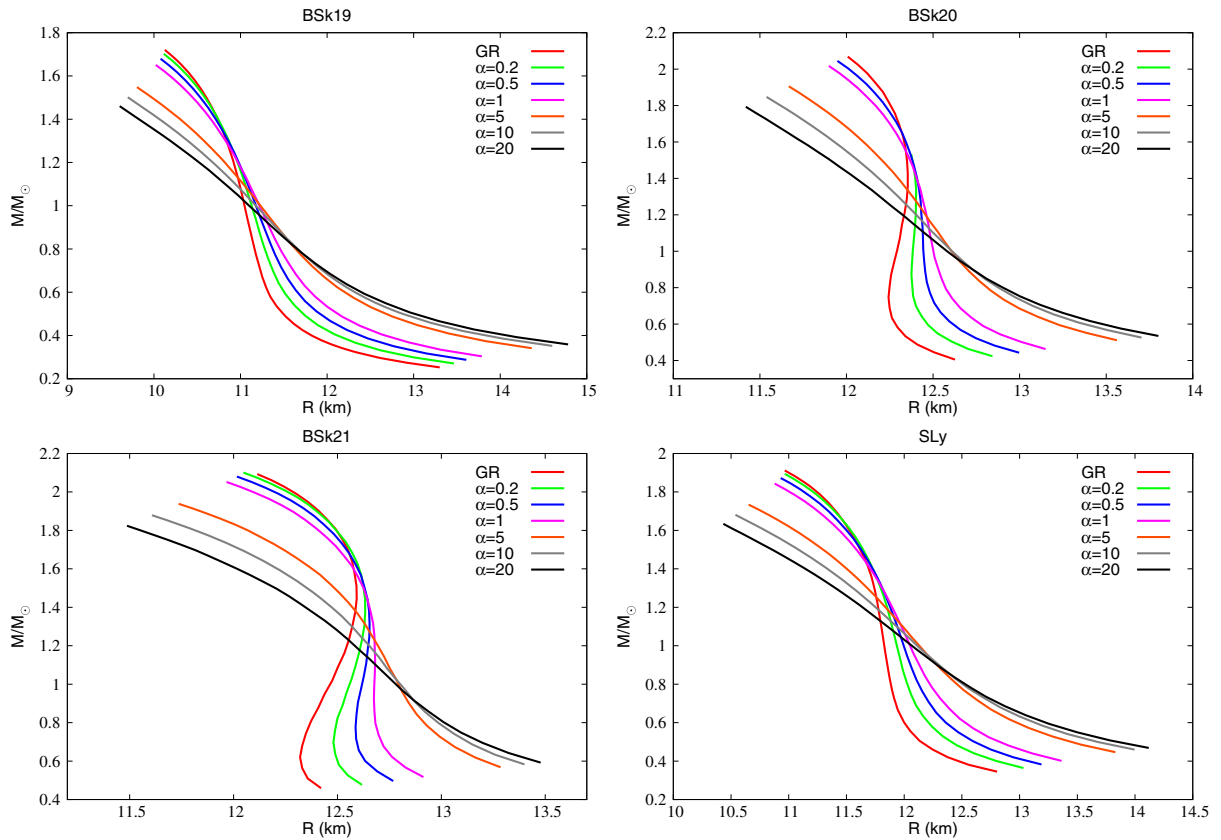

FIG. 2. $M - \mathcal{R}$ diagrams for different EoSs (labeled in the top of each panel) and quadratic form $f(R) = R + \alpha R^2$. For each EoS the maximal central density is determined by the condition $\rho_c - 3p > 0$ (see text). The classical TOV solution is also reported. The values of α are in the modulus.
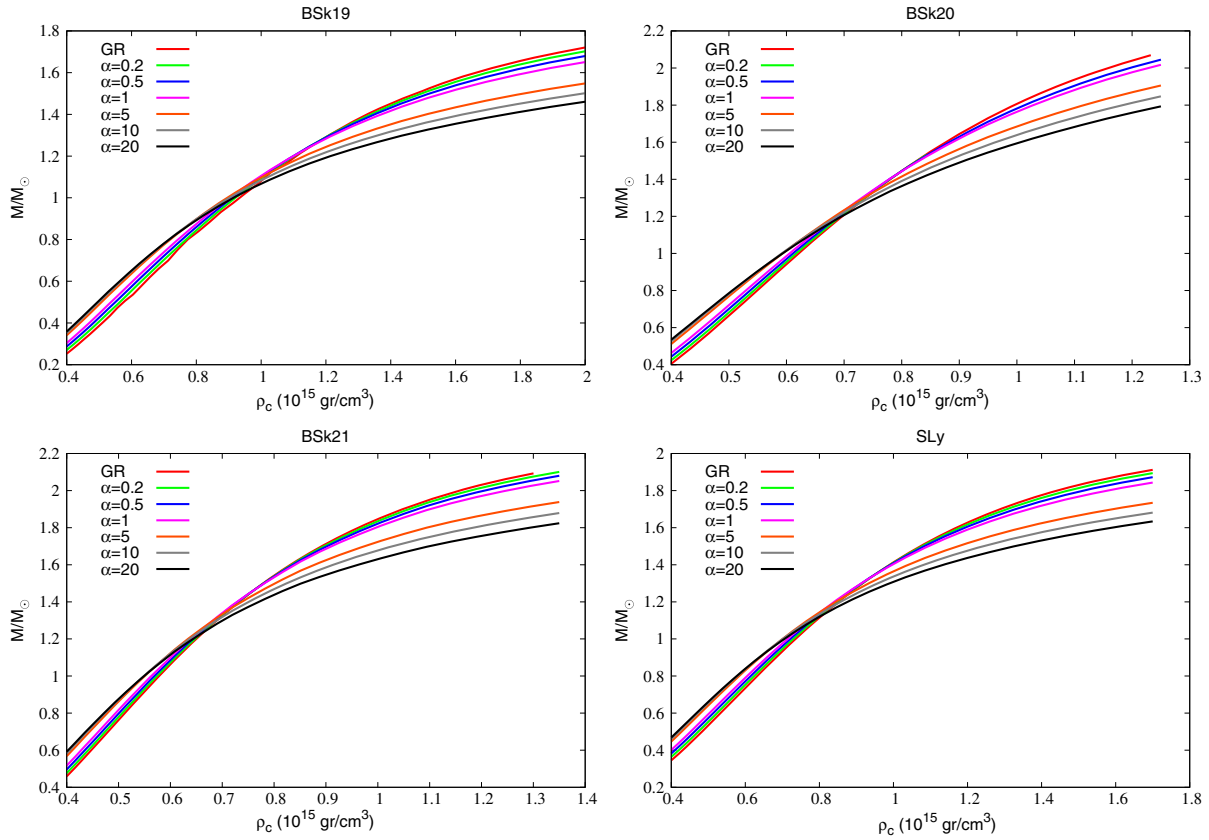
FIG. 3.   Mass versus central density for different EoSs (labeled in the top of each panel) and quadratic form $f(R) = R + \alpha R^2$. For each EoS the maximal central density is determined by the condition $\rho_c - 3p > 0$. As in Fig. 2, the modulus of α is reported (see text).

understood by keeping in mind the definition of $f(R)$ in Eq. (11), where the cubic term $\alpha\gamma R^3$ is negative for $\gamma > 0$ (being $\alpha < 0$ because of the adopted signature).

Thus, positive γ-values provide a further decrease of the value of the Lagrangian density $f(R)$ in the same fashion as the quadratic coefficient $|\alpha|$ does. This negative
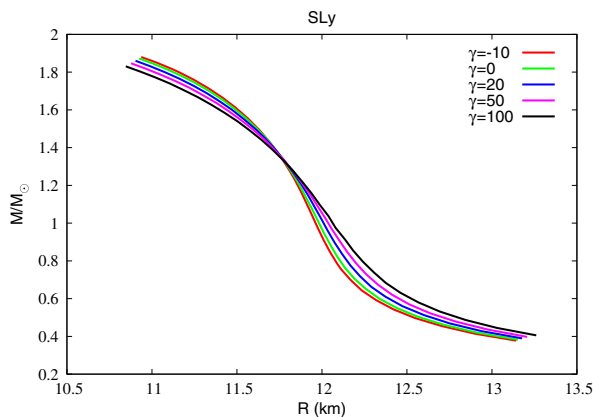

FIG. 4. $M - \mathcal{R}$ diagram for $f(R) = R + \alpha R^2(1 + \gamma R)$ with $|\alpha| = 0.5$ and different values of γ, and SLy EoS.

contribution unavoidably reflects in the $M - \mathcal{R}$ relation both for the quadratic and quadratic plus cubic corrections in R.

At the opposite, negative γ-values produce a *clockwise* rotation of the $M - \mathcal{R}$ trace. This can be seen indeed in Fig. 4 for the case $\gamma = -10$. We found however that if from one side γ can take arbitrarily negative values, this is not true in the opposite case. For instance, for the case $|\alpha| = 0.5$ and $\gamma = 20$, here discussed, we were not able to find converging solutions matching the required asymptotic behavior. As outlined above, the critical maximum value of positive γ-values depends however on the simultaneous choice of α. As an example, the combination $|\alpha| = 5\gamma = 20$ gives rise to a converging solution which is however almost indistinguishable from the case with $\gamma = 0$.

In general, we can say that for each value of $|\alpha|$, there is a critical positive value γ^{crit} above which solutions are not allowed. More specifically, for $0 \gtrsim \gamma \gtrsim \gamma^{\text{crit}}$ quadratic and cubic forms of $f(R)$ provide very similar results, while for $\gamma < 0$ it is possible to go beyond values where modifications of the $M - \mathcal{R}$ relation are more evident. In the perturbative approach both positive and negative values of γ were considered [20].
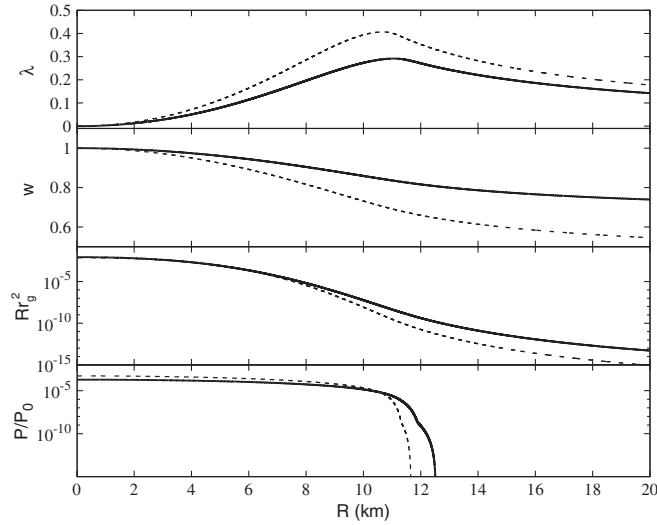
FIG. 5.   Same as in Fig. 1 but for $f(R) = R + \varepsilon R \log R$ with $\varepsilon = -0.05$.

C. Results for $f(R) = R + \epsilon R \log R$

Finally, we report the results for the model given in Eq. (15). Although the field equations given in Sec. II B are presented for clarity using the Taylor expansion for $f(R)$ of Eq. (16), it is worth noticing that we actually solved the

stellar structure equations using the exact form $f(R) = R^{1+\varepsilon}$. Similarly to Fig. 1, we show, in Fig. 5, an example of the radial behavior of the functions λ, w, R and P. The reason why we considered the case $\varepsilon \ll 1$ can be better understood by looking at the $M - \mathcal{R}$ diagram presented in Fig. 6. For $|\varepsilon| < 0.01$ a significant deviation is observed with respect to the classical TOV; at first sight, it is noticeable that the traces in the diagram present a self-similar behavior for increasing values of $|\varepsilon|$. The results of physical interest (higher masses and radii) are obtained for $\varepsilon < 0$, while, in the case of positive values of ε, the traces are blended with respect to the classical TOV solution. Note that in this case there is no pivoting around some critical central density, unlike what was found in the case of the polynomial form of $f(R)$. Actually the resizing of the action $f(R) = R^{1+\varepsilon}$ reflects in a resizing of the traces in the $M - \mathcal{R}$ diagrams. In the case of EoS BSK20 and BSK21, NS masses larger than $3M_\odot$ can be easily achieved; these values must also be considered as lower limits on the NS mass, which can be even higher for fast rotating objects.

V. DISCUSSION AND CONCLUSIONS

Neutron stars have a main role in relativistic astrophysics for several reasons. They are the most stable compact objects of the Universe (apart from black holes) where
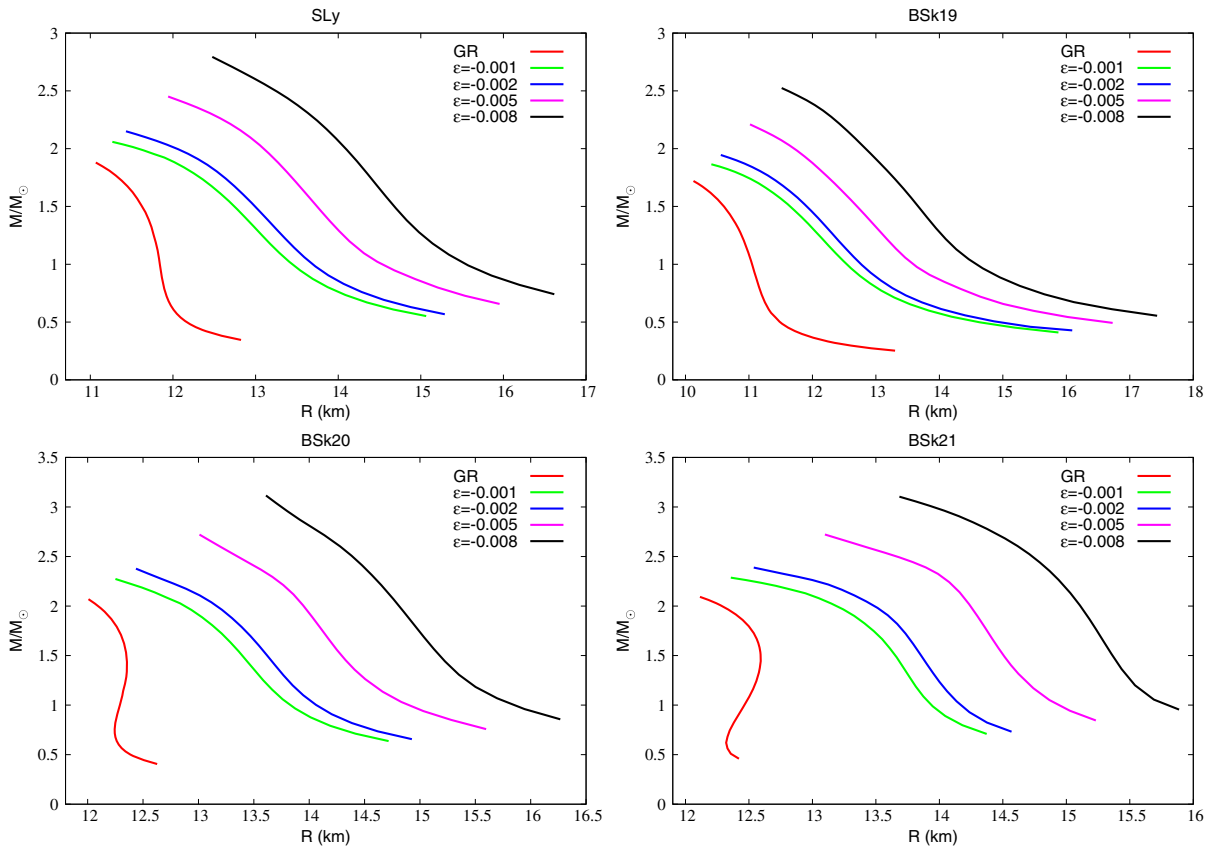

FIG. 6. $M - \mathcal{R}$ diagrams for $f(R)$ given in Eq. (15) with four EoSs and different values of ϵ. The classical TOV corresponding to $\epsilon = 0$ is also reported.

matter reaches extremely high field regimes. Also, they are very important in order to understand the final stages of stellar evolution. It is important to point out that the extreme field regimes in NS cannot be achieved in any ground-based lab so they have acquired a crucial role also in nuclear and particle physics. Due to this feature, understanding the EoS working in a NS has a twofold meaning: from one side, it can give information on the state of matter in these compact objects; on the other side, it is relevant at an astrophysical level to understand the global behavior of stars in the final stages of their life. Also, NSs could be extremely important to test alternative theories of gravity, due to the huge gravitational field acting on them.

The aim of this paper is to show that the $M - \mathcal{R}$ relation of NSs can be consistently achieved by extended theories of gravity as $f(R)$ gravity. In particular, we proposed some physically relevant $f(R)$ models and modified the TOV equations accordingly. In the stellar structure equations, new terms related to curvature corrections come out and lead the evolution of the $M - \mathcal{R}$ relation. Physically, these terms assume the role of a sort of curvature pressure capable of leading the mass and the radius of the star [20]. Specifically, we reduced the stellar structure equations to a dynamical system and integrated it numerically putting in evidence the role of curvature corrections into the integration. The resulting $M - \mathcal{R}$ diagrams strictly depend on the value of the curvature corrections, the sign of the correction parameters, and the chosen EoS. We dealt with these terms as corrections to the GR in order to control deviations with respect to the standard Einstein theory.

This point deserves a further discussion according to the numerical results presented in the above figures. Let us consider first Fig. 2, where the $M - \mathcal{R}$ relation is reported for several values of the parameter α and different EoSs. The GR value is for $\alpha = 0$ while $\alpha \neq 0$ represents corrections with respect to GR. Clearly the increasing of α in modulus gives rise to a sort of stretching-blending rotation of the $M - \mathcal{R}$ relation slope around a fixed $M - \mathcal{R}$ point that sits in the intervals $(1–1.2)M_\odot$ and $(11–12.5)$ km. This means that the magnitude of the gravitational corrections alters the structure of the NS thanks to the further curvature pressure-density terms present in the TOV equations (see also [20]). In some sense, given a EoS, curvature corrections relevantly result in shaping the stellar structure and determining the $M - \mathcal{R}$ relation. Specifically, the stretching-blending rotation depends on the effective pressure related to the curvature corrections in Eq. (6) and, in particular in Eq. (12). Increasing the parameter α means that the original $M - \mathcal{R}$ relation of GR is affected by a further pressure term that modifies the effective mass of the star and consequently its radius. However, also the effective density results are modified by the curvature corrections. Then the net effect is the stretching-blending rotation around M and $\mathcal{R}$ values where curvature corrections are not so relevant (see Fig. 2). It is important to stress again

that the stretching-bending effect is due to the curvature corrections and not to the change of the standard matter EoS.

Similar considerations hold also for the $M - \rho_c$ diagrams (Fig. 3) where the total mass of the NS is given as a function of the central density ρ_c. Also in this case we have a stretching-blending rotation around given values of mass and density (GR values) depending on the absolute value of α. If we also insert the cubic correction, led by the parameter γ, the trend is similar (see Fig. 4).

The case of $R^{1+\epsilon}$ gravity is totally different. In this case, as we can see from Fig. 6, different values of the parameter ϵ scale the $M - \mathcal{R}$ relation so that larger stable structures, in terms of mass and radius, are achieved also if slight variation with respect to the value $\epsilon = 0$ is considered. This fact could be extremely relevant in order to address extremely massive NSs as revealed by some observations [20]. Specifically, while for the quadratic and cubic models, the $M - \mathcal{R}$ relation is only modified (stretching-blending rotation) just changing the stability region of NS with respect to GR, here the curvature pressure and density give rise to a scaling law. This is quite obvious due to the $R^{1+\epsilon}$ model, but the physical consequences are relevant since extremely massive and large objects can be achieved, as one can see from Fig. 6. In such a case, the breaking of GR behavior, related to $\epsilon \neq 0$, gives rise to a new stability branch for NS allowing extreme objects. We stress again that this phenomenon is strictly related only to the effective curvature quantities and not to the change of the standard matter EoS.

It is important to stress that we never used exotic matter but only realistic EoSs. This point is crucial since we adopted always the Jordan frame so that the gravity sector results were corrected while the matter sector was unaffected. In such a way, the geodesic structure was not altered and standard EoS can be assumed. On the contrary, if we were adopting the Einstein frame, we would have the standard gravity sector but a nonminimal matter sector. In such a case, geodesic structure results were altered and it could be dangerous to adopt a standard EoS. In other words, as it is shown in detail in [43], the conformal transformations have the effect of shifting the nonminimal coupling [in our case $f'(R)^{-1}$] from the gravitational to the matter sector and then the meaning of quantities like gravitational potentials, pressure, matter density and mass results are more complicated and have to be accurately discussed. In summary, we develop our calculations in the Jordan frame considering it as the "physical" frame and avoiding the ambiguities that could emerge in the Einstein frame (see, for example, [44,45]). The same approach is adopted also in [46,47].

As an example of these considerations, we can see that, qualitatively, the behavior of the traces in the $M - \mathcal{R}$ diagrams with respect to GR is the opposite with respect to that reported by [48] for the same form $f(R) = R + \alpha R^2$ (see our Fig. 2 and Figs. 1 and 2 in [48]). The only

possibility to explain these crucial differences relies on the fact that computations in [48] were performed in the Einstein frame, while in our paper we work in the Jordan frame. The only way to compare exactly the results is to compare the behavior of the $M - \mathcal{R}$ diagram under conformal transformations assuming the same EoS. This will be the topic of the next project. Finally, the results of this work will be extended to magnetic as well as rotating neutron stars.

APPENDIX: ANALYTICAL REPRESENTATIONS OF EQUATIONS OF STATE

Here we report the functional form of the EoSs that we used in the paper to solve numerically the stellar structure equations. The pressure can be parametrized as a function of density. Let us denote with $\xi = \log(\rho/\text{g cm}^{-3})$ the dimensionless density and with $\zeta = \log(P/dyn\ \text{cm}^{-2})$ the dimensionless pressure. We used the SLy equation as reported in [49] for nonrotating NS configurations. It is

$$\zeta = \frac{a_1 + a_2\xi + a_3\xi^3}{1 + a_4\xi} f_0(a_5(\xi - a_6))$$
$$+ (a_7 + a_8\xi)f_0(a_9(a_{10} - \xi))$$
$$+ (a_{11} + a_{12}\xi)f_0(a_{13}(a_{14} - \xi))$$
$$+ (a_{15} + a_{16}\xi)f_0(a_{17}(a_{18} - \xi)), \qquad \text{(A1)}$$

where the parameters a_i for SLy EoSs are given in Table I.

For BSk19, BSk20 and BSk21, following [38], we adopted the analytical form

$$\zeta = \frac{a_1 + a_2\xi + a_3\xi^3}{1 + a_4\xi}\{\exp[a_5(\xi - a_6)] + 1\}^{-1}$$
$$+ (a_7 + a_8\xi)\{\exp[a_9(a_6 - \xi)] + 1\}^{-1}$$
$$+ (a_{10} + a_{11}\xi)\{\exp[a_{12}(a_{13} - \xi)] + 1\}^{-1}$$
$$+ (a_{14} + a_{15}\xi)\{\exp[a_{16}(a_{17} - \xi)] + 1\}^{-1}$$
$$+ \frac{a_{18}}{1 + [a_{19}(\xi - a_{20})]^2} + \frac{a_{21}}{1 + [a_{22}(\xi - a_{23})]^2}. \qquad \text{(A2)}$$

The values of parameters a_i are given in Table II.

TABLE I. Values of $a_i(\text{SLy})$ parameters for Eq. (A1).

i	$a_i(\text{SLy})$	i	$a_i(\text{SLy})$
1	6.22	10	11.4950
2	6.121	11	−22.775
3	0.005925	12	1.5707
4	0.16326	13	4.3
5	6.48	14	14.08
6	11.4971	15	27.80
7	19.105	16	−1.653
8	0.8938	17	1.50
9	6.54	18	14.67

TABLE II. Numerical values of a_i parameters for Eq. (A2).

i	a_i BSk19	BSk20	BSk21
1	3.916	4.078	4.857
2	7.701	7.587	6.981
3	0.00858	0.00839	0.00706
4	0.22114	0.21695	0.19351
5	3.269	3.614	4.085
6	11.964	11.942	12.065
7	13.349	13.751	10.521
8	1.3683	1.3373	1.5905
9	3.254	3.606	4.104
10	−12.953	−22.996	−28.726
11	0.9237	1.6229	2.0845
12	6.20	4.88	4.89
13	14.383	14.274	14.302
14	16.693	23.560	22.881
15	−1.0514	−1.5564	−1.7690
16	2.486	2.095	0.989
17	15.362	15.294	15.313
18	0.085	0.084	0.091
19	6.23	6.36	4.68
20	11.68	11.67	11.65
21	−0.029	−0.042	−0.086
22	20.1	14.8	10.0
23	14.19	14.18	14.15

[1] J. M. Lattimer and M. Prakash, Science **304**, 536 (2004).
[2] D. Psaltis, Living Rev. Relativity **11**, 9 (2008).
[3] S. Chandrasekhar, Astrophys. J. **74**, 81 (1931).
[4] S. E. Thorsett and D. Chakrabarty, Astrophys. J. **512**, 288 (1999).
[5] O. Barziv, L. Kaper, M. H. Van Kerkwijk, J. H. Telting, and J. Van Paradijs, Astron. Astrophys. **377**, 925 (2001).
[6] M. L. Rawls, J. A. Orosz, J. E. McClintock, M. A. P. Torres, C. D. Bailyn, and M. M. Buxton, Astrophys. J. **730**, 25 (2011).
[7] T. Munoz-Darias, J. Casares, and I. G. Martinez-Pais, Astrophys. J. **635**, 502 (2005).
[8] D. J. Nice, E. M. Splaver, I. H. Stairs, O. Lohmer, A. Jessner, M. Kramer, and J. M. Cordes, Astrophys. J. **634**, 1242 (2005).
[9] P. B. Demorest, T. Pennucci, S. M. Ransom, M. S. E. Roberts, and J. W. T. Hessels, Nature (London) **467**, 1081 (2010).
[10] C. E. Rhoades and J. R. Ruffini, Phys. Rev. Lett. **32**, 324 (1974).
[11] M. Nauenberg and G. Chapline, Astrophys. J. **179**, 277 (1973).
[12] S. Capozziello and M. De Laurentis, Phys. Rep. **509**, 167 (2011).
[13] S. Nojiri and S. D. Odintsov, Phys. Rep. **505**, 59 (2011).
[14] S. Nojiri and S. D. Odintsov, Int. J. Geom. Methods Mod. Phys. **04**, 115 (2007).
[15] S. Capozziello and M. Francaviglia, Gen. Relativ. Gravit. **40**, 357 (2008).
[16] S. Capozziello, M. De Laurentis, and V. Faraoni, Open Astron. J. **3**, 49 (2010).
[17] G. J. Olmo, Int. J. Mod. Phys. D **20**, 413 (2011).
[18] S. Capozziello and V. Faraoni, *Beyond Einstein Gravity: A Survey of Gravitational Theories for Cosmology and Astrophysics*, Fundamental Theories of Physics Vol. 170 (Springer, New York, 2010), ISBN 978-94-007-0164-9.
[19] S. Capozziello and M. De Laurentis, *Invariance Principles and Extended Gravity: Theories and Probes* (Nova Science Publishers, Inc., New York, 2010), ISBN 978-1-61668-500-3.
[20] A. Astashenok, S. Capozziello, and S. Odintsov, J. Cosmol. Astropart. Phys. 12 (2013) 040; Phys. Rev. D **89**, 103509 (2014); Astrophys. Space Sci. **355**, 2182 (2014); J. Cosmol. Astropart. Phys. 01 (2015) 001.
[21] P. Fiziev, Phys. Rev. D **87**, 044053 (2013); arXiv:1402.2813v1; *Proc. Sci.*, FFP14 (2014) 080; P. Fiziev and K. Marinov, Astron. J. **23**, 3 (2015).
[22] K. V. Staykov, D. D. Doneva, S. S. Yazadjiev, and K. D. Kokkotas, J. Cosmol. Astropart. Phys. 06 (2014) 003; 10 (2014) 006.
[23] N. Stergioulas, Living Rev. Relativity **6**, 3 (2003).
[24] J. R. Oppenheimer and G. Volkoff, Phys. Rev. **55**, 374 (1939).
[25] S. Weinberg, *Gravitation and Cosmology* (John Wiley & Sons, Inc., New York, 1972).
[26] A. V. Astashenok, S. Capozziello, and S. D. Odintsov, Phys. Lett. B **742**, 160 (2015).
[27] L. Rezzolla and O. Zanotti, *Relativistic Hydrodynamics* (Oxford University Press, Oxford, U.K., 2013).
[28] L. D. Landau and E. M. Lifshitz, *Fluid Mechanics,* Course of Theoretical Physics Vol. 6 (Butterworth-Heinemann, Oxford, 1987).
[29] P. A. R. Ade and PLANCK Collaboration, arXiv:1502.01590.
[30] I. L. Buchbinder, S. D. Odintsov, and I. L. Shapiro, *Effective Action in Quantum Gravity* (IOP, Bristol, U.K., 1992).
[31] N. D. Birrell and P. C. W. Davies, *Quantum Fields in Curved Space* (Cambridge University Press, Cambridge, U.K., 1982).
[32] S. Capozziello, M. De Laurentis, and M. Francaviglia, Astropart. Phys. **29**, 125 (2008).
[33] M. De Laurentis, R. De Rosa, F. Garufi, and L. Milano, Mon. Not. R. Astron. Soc. **424**, 2371 (2012).
[34] T. Clifton and J. D. Barrow, Phys. Rev. D **72**, 103005 (2005).
[35] S. Capozziello, A. Stabile, and A. Troisi, Classical Quantum Gravity **25**, 085004 (2008).
[36] S. Capozziello, M. De Laurentis, and A. Stabile, Classical Quantum Gravity **27**, 165008 (2010).
[37] J. R. Cash and A. H. Karp, ACM Trans. Math. Softw. **16**, 201 (1990); C. W. Gear and O. Sterby, ACM Trans. Math. Softw. **10**, 23 (1984); J. R. Cash, ACM Trans. Math. Softw. **15**, 15 (1989); M. W. Kutta, Zeitschrift für angewandte Mathematik und Physik **46**, 435 (1901).
[38] A. Y. Potekhin, A. F. Fantina, N. Chamel, J. M. Pearson, and S. Goriely, Astron. Astrophys. **560**, A48 (2013).
[39] J. M. Pearson, N. Chamel, S. Goriely, and C. Ducoin, Phys. Rev. C **85**, 065803 (2012).
[40] J. M. Pearson, S. Goriely, and N. Chamel, Phys. Rev. C **83**, 065810 (2011).
[41] F. Douchin and P. Haensel, Astron. Astrophys. **380**, 151 (2001).
[42] J. D. Barrow and A. C. Ottewill, J. Phys. A **16**, 2757 (1983).
[43] A. Stabile, A. Stabile, and S. Capozziello, Phys. Rev. D **88**, 124011 (2013).
[44] F. Bricese, E. Elizalde, S. Nojiri, and S. D. Odintsov, Phys. Lett. B **646**, 105 (2007).
[45] S. Capozziello, S. Nojiri, S. D. Odintsov, and A. Troisi, Phys. Lett. B **639**, 135 (2006).
[46] R. Farinelli, M. De Laurentis, S. Capozziello, and S. D. Odintsov, Mon. Not. R. Astron. Soc. **440**, 2894 (2014).
[47] S. Capozziello, M. De Laurentis, S. D. Odintsov, and A. Stabile, Phys. Rev. D **83**, 064004 (2011); M. De Laurentis and S. Capozziello, Astropart. Phys. **35**, 257 (2011); M. De Laurentis and I. De Martino, Mon. Not. R. Astron. Soc. **431**, 741 (2013).
[48] S. S. Yazadjiev, D. D. Doneva, K. D. Kokkotas, and K. V. Staykov, J. Cosmol. Astropart. Phys. 06 (2014) 003.
[49] P. Haensel and A. Y. Potekhin, Astron. Astrophys. **428**, 191 (2004).